ELSEVIER

Journal of Materials Processing Technology 54 (1995) 205–210

Journal of Materials Processing Technology

Prediction of the residual strength of laminated composites subjected to impact loading

J.Y. Huang

Aeronautical Research Laboratory, Aero Industrial Development Center, Chung Shan Institute of Science and Technology, PO Box 90008-11-3, Taichung, Taiwan, ROC

Received 1 April 1994

Industrial summary

An approximate solution of the total strain energy release rate (G) can be developed by treating impact damage as a single delamination near to the surface with an elliptical boundary. After performing the required differentiation and neglecting items of relatively small value, a concise relationship between the total strain energy release rate and the compressive strain can be obtained. By assuming the delamination implanted at the interface to have the maximum strain energy release rate, correlation with test data was obtained. To discuss the effect of the impact energy and the laminate thickness on the strain energy release rate, a parameter defined as the ratio of the impact energy to the square of the laminate thickness is introduced. Based on this analysis, it is shown the approximate solution provides a method for predicting the post-impact strength of either of thick laminate, or a thin laminate at low levels of impact energy. Various compressive failure modes induced by different impact energies, which are of importance in the prediction of residual strength, are discussed also in this paper.

Nomenclature

a	delamination size along the major axis of the ellipse
A	extensional stiffness of the sub-laminate
b	delamination size along the minor axis of the ellipse
B	coupling stiffness of the sub-laminate
D	bending stiffness of the sub-laminate
E_{11}	Young's modulus in the fiber direction
E_{22}	Young's modulus in transverse direction
G_{12}	shear modulus
G^a	strain energy release rate along the major axis
G_{IC}	inter-laminar fracture toughness
h	thickness of the sub-laminate
M	force per unit length of the cross-section of the sub-laminate
N	moment per unit length of the cross-section of the sub-laminate
t	laminate thickness
U	total strain energy of the sub-laminate
V	potential energy
u_1	displacement component in the x-direction
u_2	displacement component in the y-direction
w	displacement component in the z-direction

Greek symbols

ε	in-plane strain
ε_0	far-field compression strain in the parent laminate along the x-direction
κ	curvature
ν	Poisson's ratio of the parent medium
γ	ratio of the impact energy to the square of the laminate thickness
Π	total potential energy

1. Introduction

Laminated composites, with their high strength-to-weight ratio, offer considerable technological advantages in the production of aircraft and other applications. However, the design involved is complex, due to the inhomogeneous nature of the material and its failure modes. It has been agreed widely that the worst damage arising during the service of the composite material is delamination caused by low-velocity impact of foreign objects. Under buckling, there appears a high inter-laminar stress at the delamination front that leads to a spreading of the delamination, which can significantly

SSDI 0924-0136(95)01943-9

reduce the compressive strength and stiffness of the laminate. Furthermore, buckling is accompanied by an instantaneous fracture of the inter-laminate bond. Many investigations have been made on the impact test and on the damage-stability mode of composite materials [1–3]. Unfortunately, the state of impact damage in the laminate is so complex that the distribution of the delamination depth is difficult to reveal non-destructively. However, as it is the surface layer that in most cases is damaged, assumption can be made by simplifing the impact damages to a single delamination near to the surface with an elliptical boundary. Moreover, the delaminated sub-laminate is thin compared to the parent laminate, so that thin-film assumptions can be applied.

Post-buckling solution for a 2-dimensional elliptical delamination was obtained using the Rayleigh–Ritz technique combined with Von-Karman finite-deflection strain by Chai [2]. The problem of the buckling of a thin laminated surface layer had been considered as a classical linear problem of buckling of a strip with fixed ends [4]. In this article, the strain energy release rate of the embedded delamination using the thin-film assumptions and the much simpler displacement expression, is derived as a function of parameters including the delamination major axis a, minor axis b, the external compressive strain, Poisson's ratio of the parent laminate, and the extensional and bending stiffnesses of the sub-laminate. Correlating the analyzed G value with the test data, the relationship between these parameters is discussed.

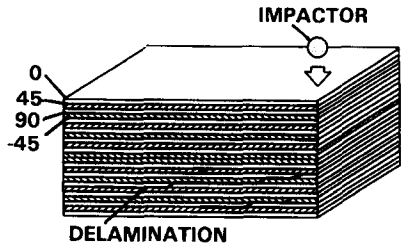

Fig. 1. Delamination distribution along the 0° fiber direction of an impacted laminate revealed by the deplying technique. (A quarter specimen is shown).

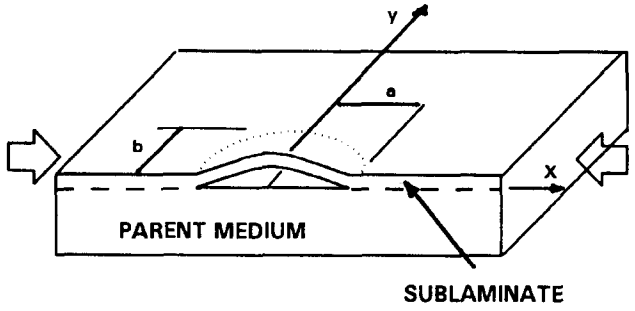

Fig. 2. Geometry and boundary condition of an embedded delamination.

2. Analysis

Based on the results of impact tests, the major damages are usually observed near to the surface on the rear face of the impacted laminate, as shown in Fig. 1.

The buckled region, as indicated in Fig. 2, is referred to as the "sub-laminate". The thick plate, referred to as the "parent medium", can be regarded as an isotropic material. Since the thickness of the sub-laminate is assumed to be small compared to that of the parent medium, thin-film assumptions can be applied. The appropriate boundary conditions are

$$w = 0, \qquad \frac{\partial w}{\partial n} = 0 \quad \left(\text{for } \frac{x^2}{a^2} + \frac{y^2}{b^2} = 1\right), \tag{1}$$

where n is the normal to the plate boundary. These conditions are satisfied if the following expression [5] is assumed for the deflection:

$$w = w_0\left(1 - \frac{x^2}{a^2} - \frac{y^2}{b^2}\right)^2, \tag{2}$$

where w_0 is the deflection at the middle of the ellipse, and a, b are the delamination sizes along the major axis and minor axis, respectively. Kachanov [4] calculated the value w_0 by considering the length contraction due to bending equal to the length contraction due to compression before buckling. In other words, the length does not change in buckling. In this the present work, the in-plane displacement in the x direction at the clamped type boundary of the ellipse is assumed to consist of two parts: u_1 and u_2, where u_1 is the shortening due to the compression in the parent medium and u_2 is the in-plane displacement at boundary of ellipse, parallel to the x-axis, which arises form the length variation due to the buckling of the ellipse. Assuming that the state of stress in the parent medium remained unaltered the during buckling stage of the disbonded region, u_1 can be assumed as [2]

$$u_1 = -\varepsilon_0 a\sqrt{(1-(y/b)^2)}, \tag{3}$$

where ε_0 is far-field compression strains in the parent medium along the x-direction. u_2 can be obtained as follows:

$$u_2 = \frac{1}{2}\int_0^s \left(\frac{\mathrm{d}w}{\mathrm{d}x}\right)^2 \mathrm{d}x = 0.61(w_0/a)^2[1-(y/b)^2]^{7/2}, \tag{4}$$

where $s = b\sqrt{1-(y/b)^2}$. By combining the displacement in Eqs. (3) and (4), the in-plane displacement parallel to the x-axis at the boundary of the ellipse is obtained, and by assuming the displacement u within the ellipse to be linear in x [2,6]:

$$u = \{-\varepsilon_0 + 0.61(w_0/a)^2[1-(y/b)^2]^3\}\,x. \tag{5}$$

Similarly, the in-plane displacement parallel to the y-axis is

$$v = \{v\varepsilon_0 + 0.61(w_0/b)^2[1-(x/a)^2]^3\}y. \quad (6)$$

The total potential energy, Π, of the sub-laminate is the sum of the strain energy U and the potential energy V:

$$\Pi = U + V. \quad (7)$$

The strain energy of the delaminated sub-laminate region is

$$U = \frac{1}{2}\int_{-a}^{a}\int_{-s}^{s}\begin{Bmatrix}\varepsilon\\ \kappa\end{Bmatrix}^{\mathrm{T}}\begin{bmatrix}N\\ M\end{bmatrix}\mathrm{d}x\,\mathrm{d}y$$
$$= C_4 w_0^4 + C_3 w_0^3 + (C_2 + C_e\varepsilon_0)w_0^2 + C_0\varepsilon_0^2, \quad (8)$$

where

$$C_4 = 0.078\pi(b^4A_{11} + a^4A_{22} + 1.27a^2b^2A_{66} + 0.624b^4A_{11})/a^3b^3,$$
$$C_3 = 1.07\pi(B_{12} + 2B_{66})/ab,$$
$$C_2 = 4\pi((b/a)^2D_{11} + (a/b)^2D_{22} + (2/3)(D_{12} + 2D_{66}))/ab,$$
$$C_0 = (\pi ab/2)(A_{11} - 2vA_{12} + v^2A_{22}),$$
$$C_e = (-\pi/3)(A_{11} - v(a/b)^2A_{22} + ((a/b)^2 - v)A_{12})(b/a), \quad (9)$$

where N and M are the force and moment per unit length of the cross-section of the sub-laminate, respectively. The A, B and D matrices denote the extensional, coupling and bending stiffness of the delaminated plies, respectively. The potential energy V of the stress resultants is given by [7]

$$V = \frac{1}{2}\int_{-a}^{a}\int_{-s}^{s}\{N_x(w_{,x})^2 + N_y(w_{,y})^2 + 2N_xy(w_{,x}w_{,y})]\,\mathrm{d}x\,\mathrm{d}y = T_e\varepsilon_0 w_0^2 \quad (10)$$

The unknown parameter w_0 can be determined by applying the Trefftz criterion [7], i.e.:

$$\partial^2\Pi/\partial w_0^2 = 0, \quad (11)$$

which yields

$$w_0 = \frac{-3C_3 + \sqrt{9C_3^2 - 32C_4(C_2 + C_e\varepsilon_0)}}{8C_4}, \quad (12)$$

For w_0 to be real, the buckling strain of the ellipse is derived as

$$\varepsilon_{cr} \leqslant \frac{9C_3^2}{32C_4C_e} - \frac{C_2}{C_e}. \quad (13)$$

The strain energy release rate along the major and minor axis is given as [2]

$$G^\alpha = -\frac{\alpha}{\pi ab}\frac{\partial U}{\partial \alpha} + G_0, \quad (14)$$

where $\alpha = a, b$, and $G_0 = C_0\varepsilon_0^2/ab$ denotes the membrane strain energy per unit area released from the newly delaminated portion of the sub-laminate.

By neglecting those items in Eqn. (14) with relatively small values, the approximate strain energy release rate along the major axis can be expressed as a function of the delamination major axis and minor axis, the external compressive strain, Poission's ratio of the parent laminate, and the extensional and bending stiffnesses of the sub-laminate:

$$G^\alpha = \beta_1\varepsilon_0^2 + \beta_2\varepsilon_0^{3/2} + \beta_3\varepsilon_0 + \beta_4\varepsilon_0^{1/2} + \beta_5 + \beta_6/\varepsilon_0^{-1/2}, \quad (15)$$

where

$$\beta_1 = 0.036A_{11}^2(A_{11} + 6\alpha^4A_{22})/a^2f^2,$$
$$\beta_2 = 1.7aA_{11}^{3/2}g(A_{11} - 3.5\alpha^4A_{22})/f^{5/2},$$
$$\beta_3 = A_{11}[35.6g^2(a/b)^3 - 1.75D_{11}(A_{11} + 3.5\alpha^4A_{22})/a^2]/f^2,$$
$$\beta_4 = -7.6gA_{11}^{1/2}D_{11}(A_{11} + 2\alpha A_{22})/ab^2f^{5/2}$$
$$\beta_5 = 25D_{11}^2(A_{11} + 2\alpha^2A_{22})/a^4f^2 - 343D_{11}g^2(A_{11} - 3\alpha^4A_{22})/b^4f^3,$$
$$\beta_6 = 363D_{11}g(A_{11} + 2\alpha^4A_{22})[2\alpha^4g^2 + D_{11}(A_{11} + \alpha^4A_{22})]/a^3b^2A_{11}^{1/2}f^{7/2},$$
$$f = (A_{11} + \alpha^4A_{22}),$$
$$g = (B_{12} + 2B_{66}),$$

3. Experimental

The mechanical properties of material T300/976 were given as follows:

$$E_{11} = 131\,\mathrm{GPa},$$
$$E_{22} = E_{33} = 7\,\mathrm{GPa},$$
$$G_{12} = G_{13} = G_{23} = 4.3\,\mathrm{GPa},$$
$$v_{12} = v_{13} = v_{23} = 0.3,$$
$$G_{IC} = 228\,\mathrm{J/m^2}\text{: interlaminar fracture toughness.} \quad (16)$$

Subscripts 1, 2 and 3 correspond to the longitudinal, transverse and thickness direction, respectively, of a zero-degree lamina. The test specimens are 152 mm × 102 mm composite plate. A falling-weight impact tester with a 12.7 mm hemispherical steel tip impactor was used to perform the impact test. Four firmly-fixed edges of the plates were applied to simulate a "clamped" boundary.

The impact energies can be controlled by adjusting the height and weight of the striker. After impact, an ultransonic C-scan was utilized to determine the extent of the internal damage of the specimen. To investigate the distribution of the delamination damage, the specimens were cut along the 0° directions through the impacted regions, the cross-section then being polished and examined by optical microscope. Post-impact compression tests with an anti-buckling guide were performed to measured the residual compressive strengths. The experimental details can be found in [8].

4. Result and discussion

4.1. Buckling strain

Considering a strip delamination i.e., the limiting case $b \gg a$, in an isotropic plate, the above buckling strain in Eq. (13) reduced to

$$\varepsilon_{cr} = \frac{2}{(1-\nu^2)}\left(\frac{h}{2a}\right)^2, \tag{17}$$

which has the same form as the solution given in [7]. Here, h denotes the thickness of the sub-laminate. The reason why the coefficient of Eq. (17) is not equal to $\pi^2/3$ as in [9] is due to the selection of the function of w. If the deflection is assumed to be $w = w_0[1-(x/a)^2-(y/b)^2][1+w_1((x/a)^2+(y/b)^2)]$, a buckling strain with the same function form but with a different coefficient will be obtained. The relation between ε_{cr} and Poisson's ratio of the parent medium, ν, can be investigated from Eq. (13). For a larger values of ν, the critical buckling strain ε_{cr} becomes greater. Furthermore, the buckling strain ε_{cr} increases with increase in sub-laminate thickness.

4.2. Post-impact residual-strength prediction

Laminates with a lay-up of $[(0/45/90/-45)_n]_s$, $n = 2, 3, 4, 6, 9$ were selected for the CAI (Compression After Impact) test, the test results of laminate $[(0/45/90-45)_4]_s$ being listed in Table 1. For simplicity, a single elliptical delamination is assumed to be implanted at the interface near to the surface of a quasi-isotropic laminate $[(0/45/90/-45)_n]_s$ to simulate the impact damage. The critical strain energy release rates were back-calculated by substituting the test data of the residual strains into Eq. (14). Delamination growth, characterized by the fracture-mechanics concept, was assumed to occur when the strain energy release rate G^a exceeded the energy required to spread the delaminated area. By assuming that growth of the delamination will cause global failure of the laminate, the interface having the maximum strain energy release rate was selected to correlate the approximate solution with the CAI test data. The plot of critical strain energy release rates versus square of strains calculated from residual strength is shown in Fig. 3.

To discuss the effect of impact energy and laminate thickness on the strain energy release rates, a parameter γ, which is the ratio of impact energy to the square of the laminate thickness, is introduced as shown in Fig. 4.

Data with the ratio less than $3.0 * 10^5$ J/m^2 are shown by a star "*" mark in Fig. 3, and tend to construct a constant G_c group. Thus, for either thick laminate, or thin laminate at small impact energy, as long as the ratio γ is less than $3.0 * 10^5$ J/m^2 the approximate solution can be used to predict the residual strength after impact. Here, the constant G_c shown in Fig. 3 is very close to the tested critical inter-laminar strain energy release rate of 228 J/m^2.

That the approximate solution is no longer valid for predicting the post impact residual strength when the ratio γ exceed $3.0 * 10^5$ J/m^2 can be explained by the following:

(1) Since the thickness of the sub-laminate is assumed to be small compared to that of the parent medium, the assumption of a thin-film becomes invalid for a thin laminate.

(2) For a laminate impacted at small energy, the compressive failure mode of the laminate is consistent with the analysis model, i.e. the delamination continue to spread in one main interface until the laminate separate into two sub-laminates, whilst for a laminate impacted at high energy, a shear-type failure mode is dominant, as shown in Fig. 5, indicating that matrix-cracking damage is significant. In this case, the model of a single delamination used for calculating the approximate solution is unsuitable.

Table 1
Impact test results of laminate $[(0/45/90/-45)_4]_s$

Specimen	1	2	3	4	5	6
Weight of Impactor (kg)	1.85	1.85	1.85	1.85	1.85	1.85
Height of Impactor (m)	0.50	0.56	0.53	0.45	0.39	0.34
$2a$ (mm)	38	51	30	38	38	28
$2b$ (mm)	20	25	23	23	23	23
Residual strength (MPa)	177	179	179	194	202	245

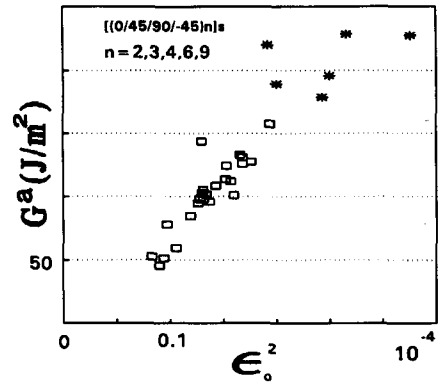

Fig. 3. Critical strain vs. maximum strain energy release rates.

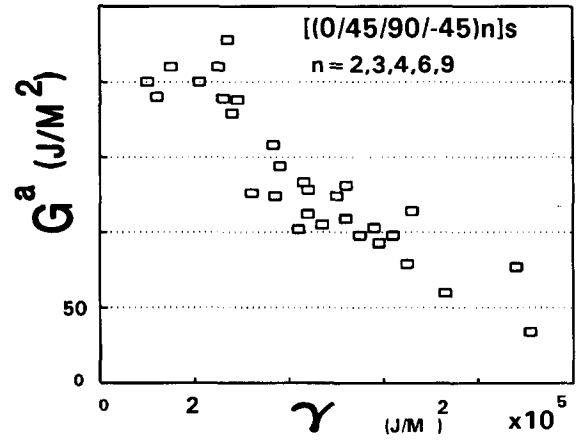

Fig. 4. G vs. γ (impact energy/square of laminate thickness).

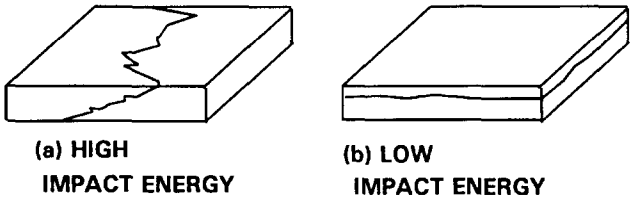

Fig. 5. Compressive fracture modes of laminates impacted at different levels of energy:

This apsect can be further explained by investigating the load–displacement diagram of the compressive test, as shown in Fig. 6.

For a laminate impacted at lower impact energy, the compressive force is linear with displacement until final collapse occurs, whilst for a laminate at higher energy, a zig-zag phenomenom is obtained, which can be explained as the coalescence process of damages.

(3) Examining the coefficients of the approximate solution has shown that when β_5 and β_6 in Eq. (15) becomes significant, the strain energy release rate is no longer controlled by coefficient β_1. In this case, the relationship between G and square of strain as shown in Fig. 3 will not be linear, i.e., a constant value of G_c is possible.

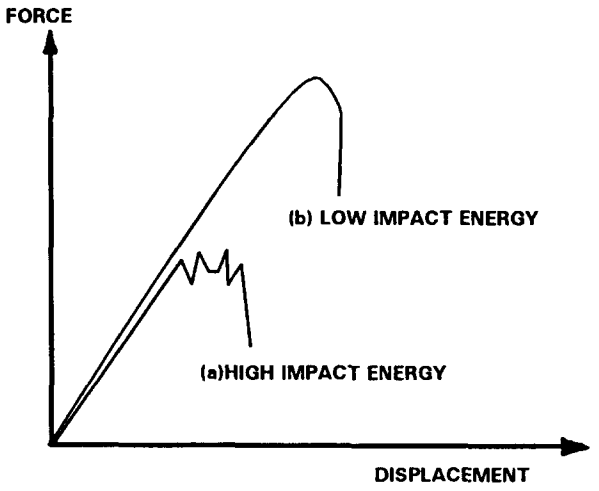

Fig. 6. The load–displacement diagram of the compressive test for laminates impacted at different energy.

To make the coefficient β_5 and β_6 of a thin laminate become significant, the damage should usually be kept small, in other words, a small impact energy is required. For a thick laminate, the delamination is usually assumed to be embedded in a deeper interface, which gives a larger value of D_{11}. In this case, β_5 and β_6 also become of larger value. This explains why the approximate strain energy release rates will only become independent of the compressive strain either for a thick laminate, or a thin laminate at low levels of impact energy.

5. Conclusions

The conclusions from this work can be summarized below:

1. The buckling strain of the sub-laminate influenced by the Poisson's ratio of the parent medium and the thickness of the sub-laminate.
2. The approximate solution provides a method for predicting the post-impacted strength of a composite laminate for only either a thick laminate or a thin laminate with at low impact energy.
3. Various compressive failure modes were induced by different impact energies which are of importance in prediction the residual strength of a laminate after impact.

References

[1] S. Abrate, Impact on laminated composite materials, *Appl. Mech. Rev.*, 44 (1991) 155.
[2] H. Chai and C.D. Babcock, Two-dimensional modelling of compressive failure is delaminated laminates, *J. Composite Mat.*, 19 (1985) 67.
[3] D. Liu, L.S. Lillycrop, L.E. Malvern and C.T. Sun, The evaluatin of delamination – an edge replication study, *Exp. Tech.*, 11 (5) (1987) 20.

[4] L.M. Kachanov, *Delamination Buckling of Composite Materials*, Kluwer, Dordrecht, 1988.
[5] A.C. Ugural, *Stresses in Plates and Shells*, McGraw-Hill, New York, 1981.
[6] K.N. Shivakumar and J.D. Whitcomb. Buckling of a sublaminate in a quasi-isotropic composite laminate, *J. Composite Mat.*, 19 (1985) 2.
[7] J.E. Ashton and J.M. Whitney, *Theory of Laminated Plates*, Progress in Materials Science Series, Vol. IV, Technomic, Lancaster, 1970.
[8] C.L. Ong, M.F. Sheu, Y.Y. Liou and T.J. Hsiao, The study of the characteristics of composite after impact, *SAMPE Int. Symp.*, 36 (1991) 912.
[9] H. Chai, C.D. Babcock and W.G. Knauss, One-dimensional modelling of failure in laminated plate by delamination buckling, *Int. J. Solids Struct.*, 17 (11) (1981) 1069.